Hierarchical joint classification models for multi-resolution, multi-temporal and multi-sensor remote sensing images. Application to natural disasters

Ihsen HEDHLI [§*]

In collaboration with

Gabriele Moser[§], **Sebastiano B. Serpico**[§] **and Josiane Zerubia**[*]

Publications available on https://team.inria.fr/ayin/publications-hal/

*

§

Introduction and Background

Remote sensing and applications

Remote sensing has extensive applications:

Mineral exploration

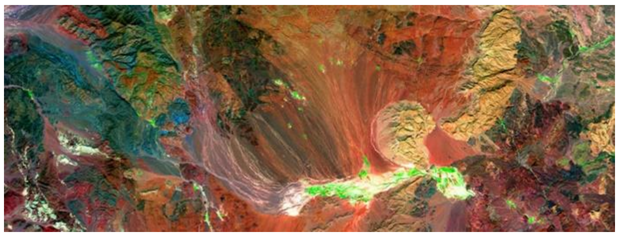

Weather prediction

Risk management

Precision agriculture

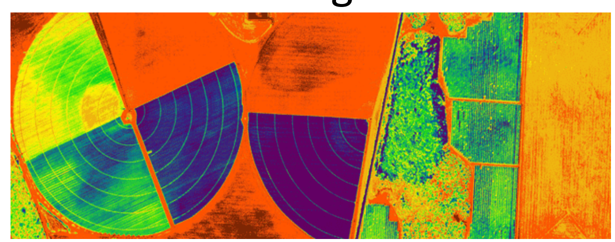

Infrastructure management

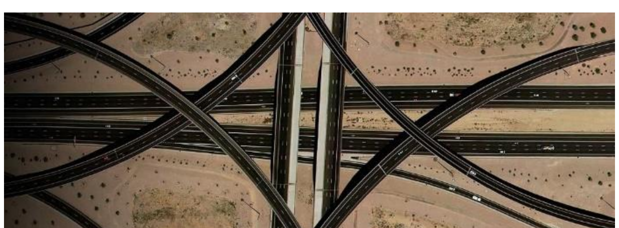

Urban mapping

Introduction and Background

Remote sensing and applications

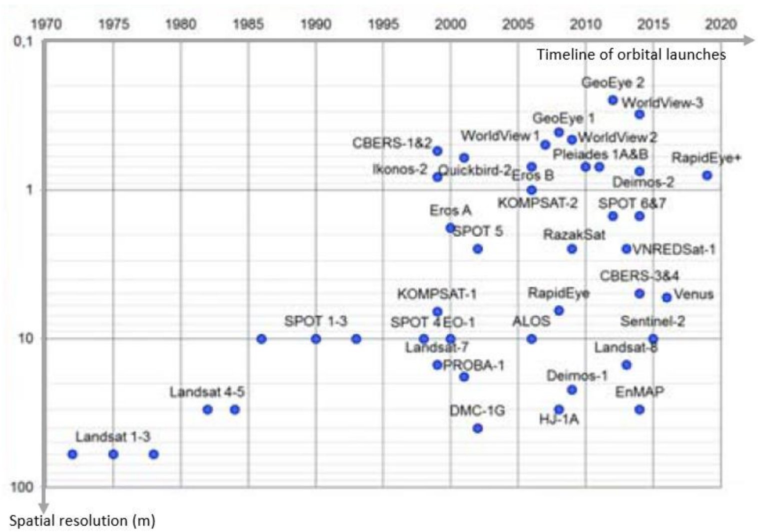

Systems operating in optical spectrum

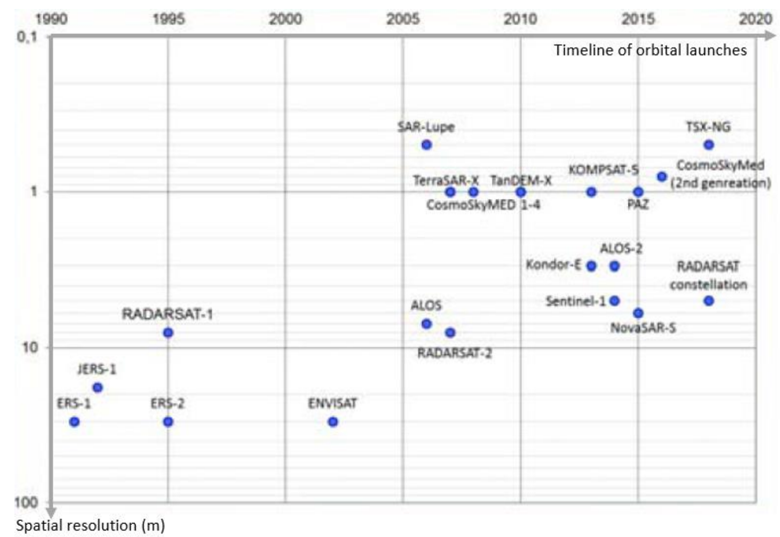

Systems operating in microwave spectrum

The **proliferation** of data gives rise to the increasing complexity of RS data,
As well as to the **diversity** and **higher dimensionality** characteristic of the data.

Complementary informations

Introduction and Background

Remote sensing data

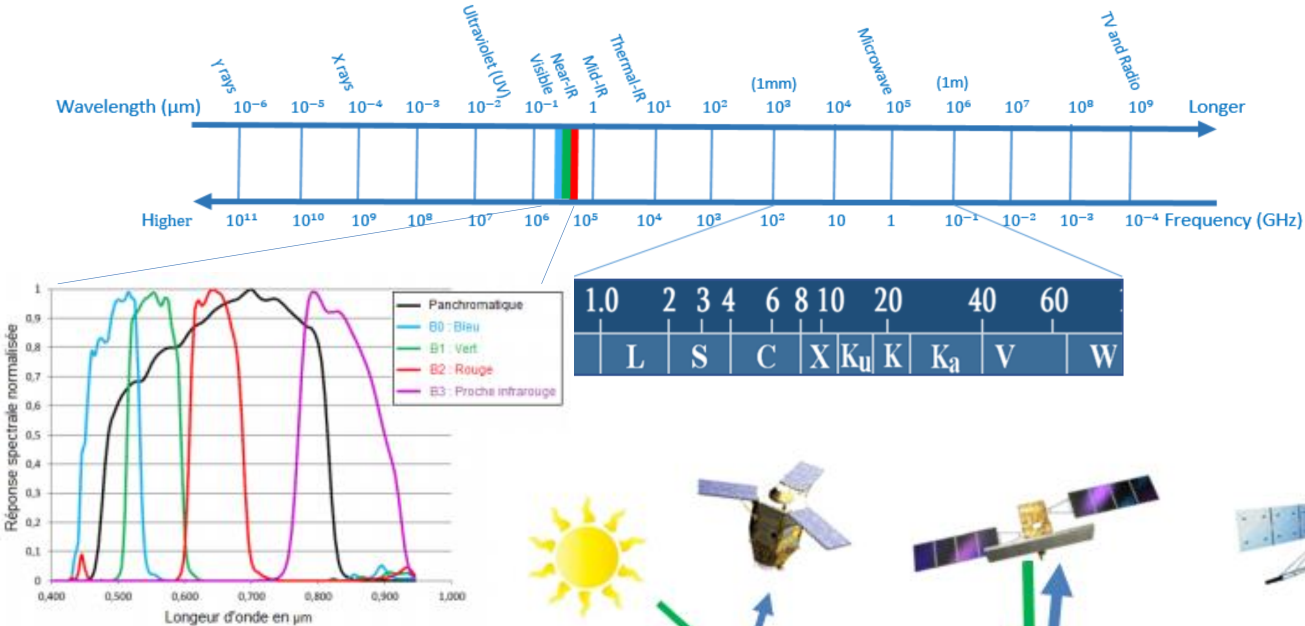

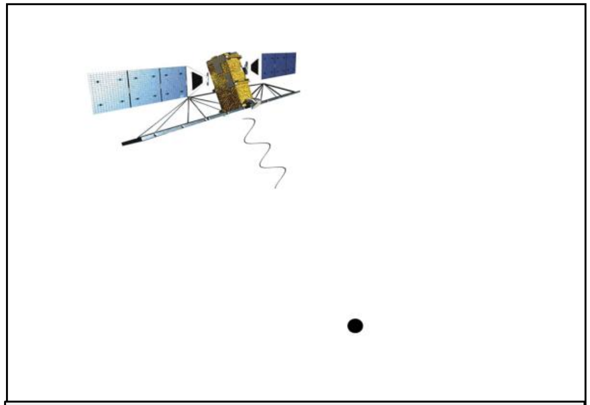

Scattering intensity has a strong dependence on the size of the particles

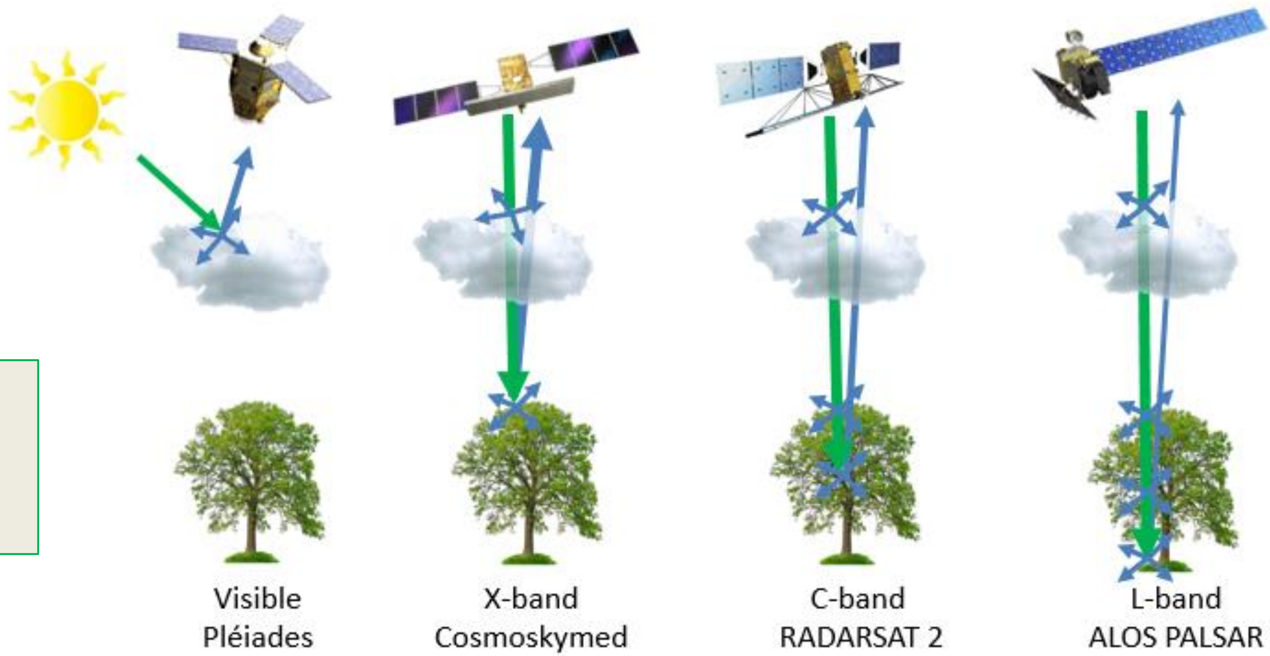

! valuable spatial information from different sensors

Introduction and Background

Focus on image classification as part of risk management

Risk management

Earthquake in Nepal (2015)

Introduction to the Research Activity

Focus of the talk

Due to the huge number and the (short) revisit time of high resolution satellites

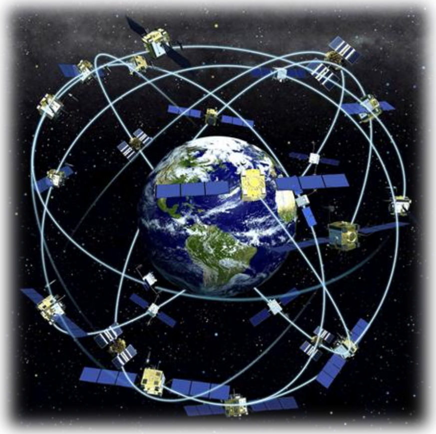

Huge amount of satellite images can be acquired at different resolutions

valuable spatio-temporal information.

Problem Statement

develop methods to explore such huge data

- Multiresolution information
- Multitemporal information
- Multisensor information

Introduction to the Research Activity

Objectives

- ✓ Joint classification of coregistered mono-/multi-band, multi-resolution and/or multi-sensor (SAR, optical) acquisitions into M *classes.*
- ✓ Hierarchical graph: use multi-resolution data.
- ✓ Flexible enough and sufficiently robust to different types of images at different dates and/or from different sensors.

Key points

- ✓ Focus on multi-resolution and multi-temporal optical images
- ✓ Extension to multi-sensor images (SAR+ optical) and multi-frequency SAR

Proposed methods

Three novel hierarchical methods have been proposed to fuse multi-date, multi-resolution, multi-band and multi-sensor remote sensing imagery for multi-temporal classification purposes. Experimentally validated with challenging multi-modal imagery from Haiti test sites

Contents

Contents

Hierarchical Markov Model on quad-trees

General presentation: Hierarchical method

❖**Classification**: **Estimate the labels X *at the finest resolution* given all the observations.**

❖**Quad-tree structure**: **causality that allows to use a non-iterative algorithm.**

❖**MPM (Marginal Posterior Mode) criterion**: **penalizes the errors according to their number and the scale at which they occur.**

Hierarchical Markov Model on quad-trees

Causality

- Define an **order** over the set of sites S. In such a way, we characterize the past of a site $s(i,j)$
- For instance:

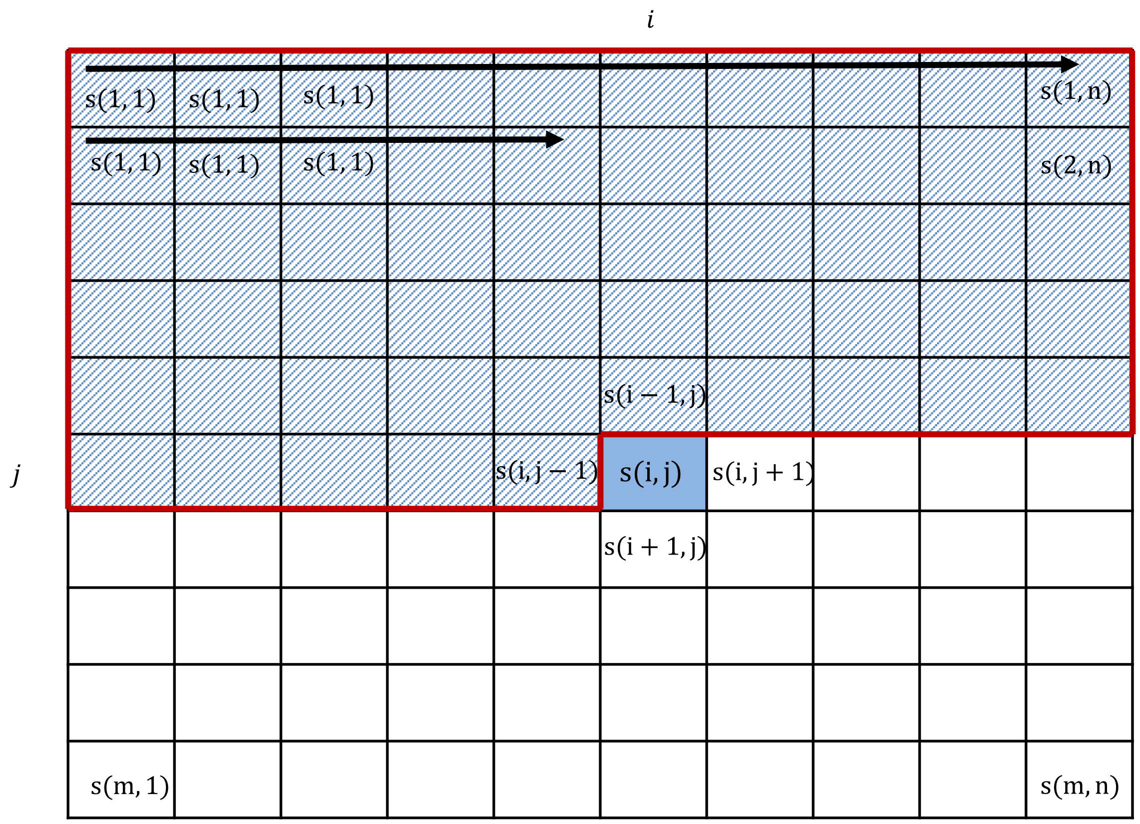

Hierarchical Markov Model on quad-trees

Pyramid structure

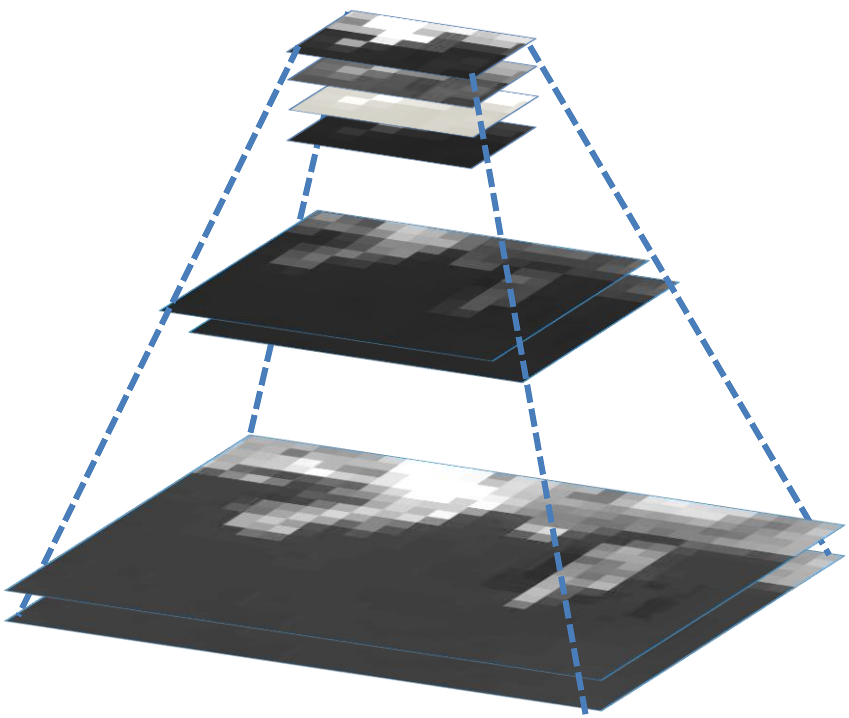

Pléiades sensor

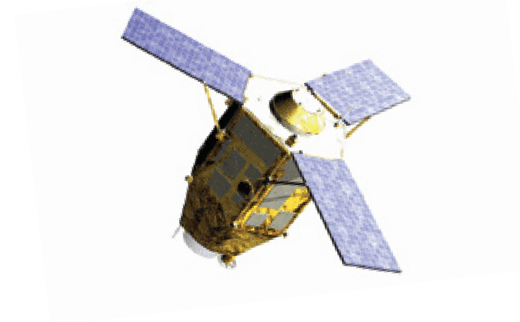

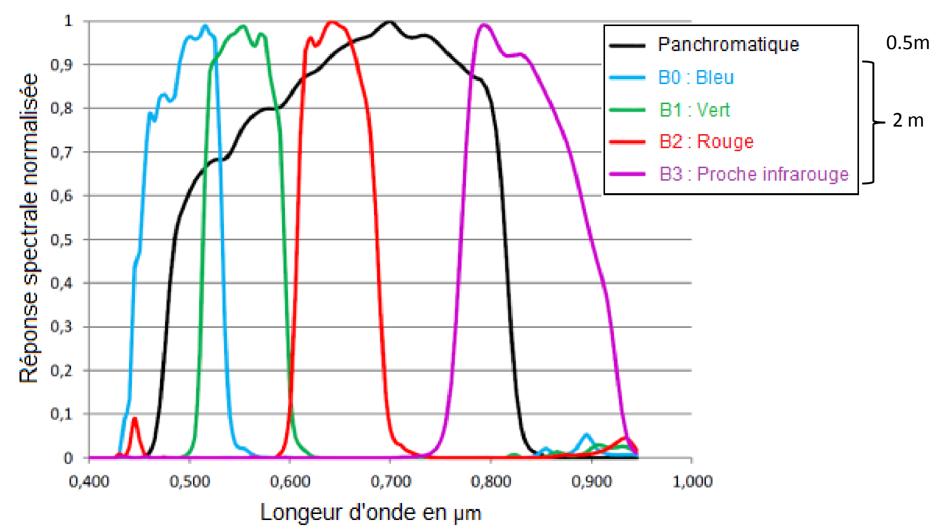

- Images are organized according to their resolutions in a pyramid structure

Hierarchical Markov Model on quad-trees

Quad-tree structure

Missing levels might appear

wavelets

Operators on the quad-tree :

- δ : the backward shift
- α : the interchange operator at the same scale
- β : the forward shift

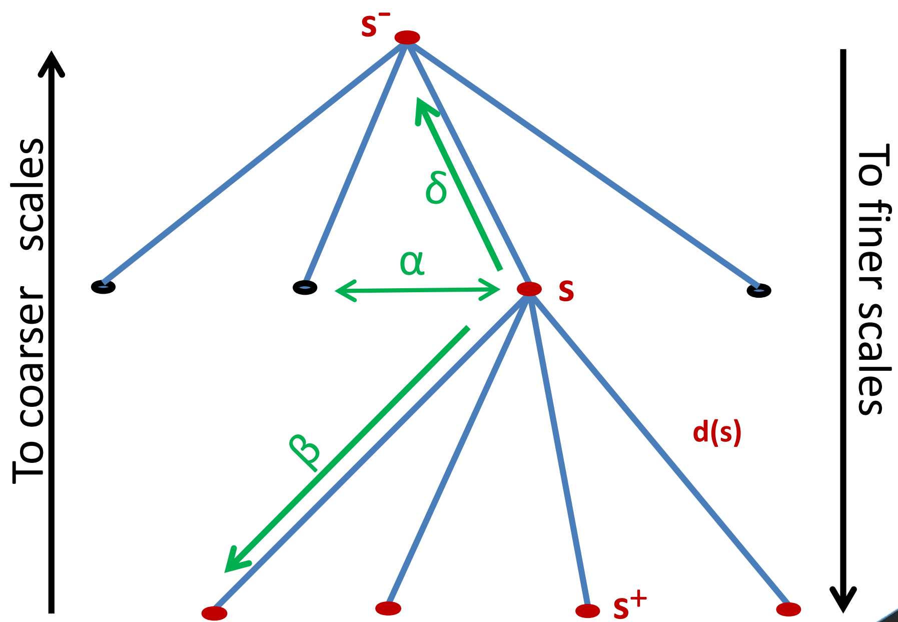

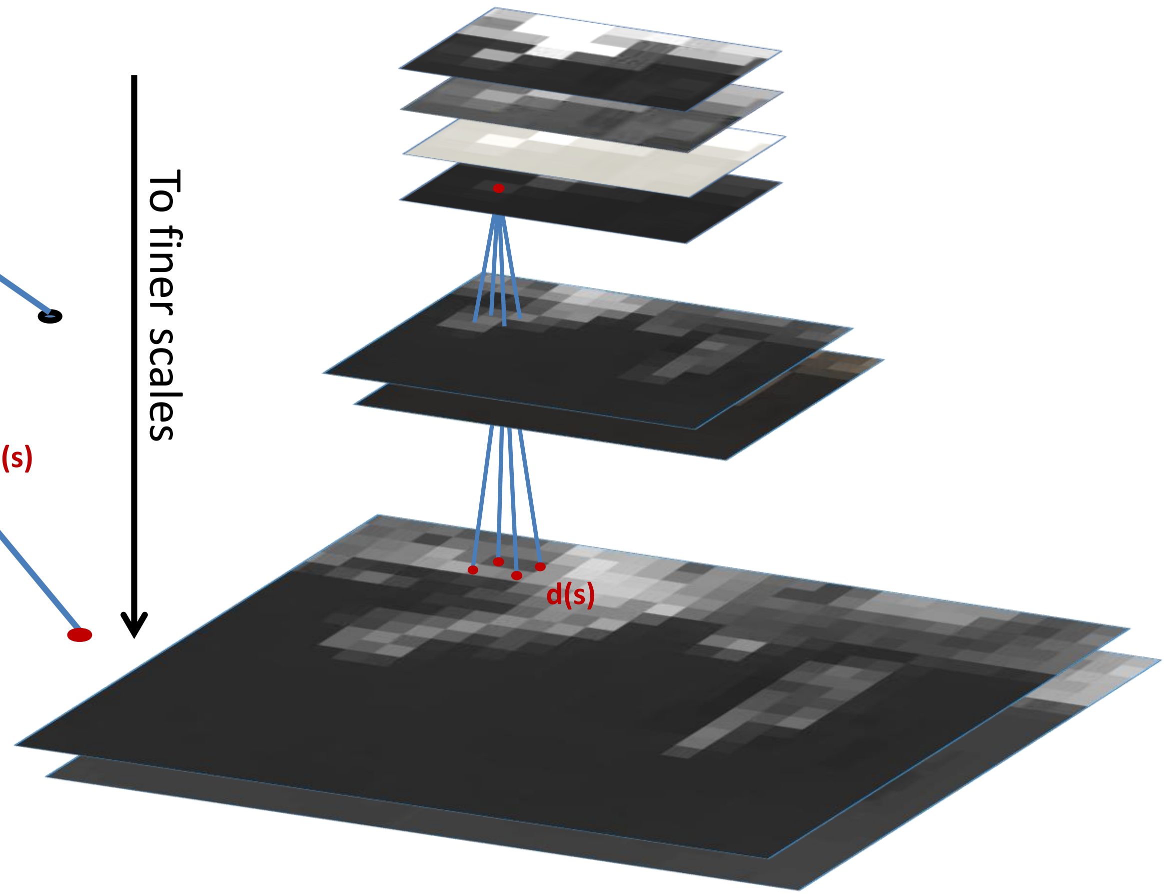

- $s^- = \delta(s)$
- $s^+ = \beta(s)$
- $d(s) = s^+ \cup (s^+)^+ \cup ((s^+)^+)^+ \cup \ldots$

Hierarchical Markov Model on quad-trees

MPM criterion

$$\boxed{\hat{x}_s = arg \max_{x_s \in \omega} P(x_s | y)}$$

$$p(x_s | y) = \sum_{x_{s^-}} \left[\frac{p(x_s, x_{s^-} | y_{d(s)})}{\sum_{x_s} p(x_s, x_{s^-} | y_{d(s)})} . p(x_{s^-} | y) \right]$$

Calculate recursively the posterior marginal $p(x_s | y)$ while the probabilities $p(x_s, x_{s^-} | y_{d(s)})$ are made available.

$$\frac{\overset{3}{p(x_s | x_{s^-})} . p(x_{s^-})}{\underset{1}{p(x_s)}} . \overset{2}{p(x_s | y_{d(s)})}$$

1 Prior

2 Posterior marginal

3 Transition Probabilities over scale

These probabilities are calculated through a MPM algorithm which runs in two passes on a quad tree, referred to as "bottom-up" and "top-down" passes.

Hierarchical Markov Model on quad-trees

Global scheme

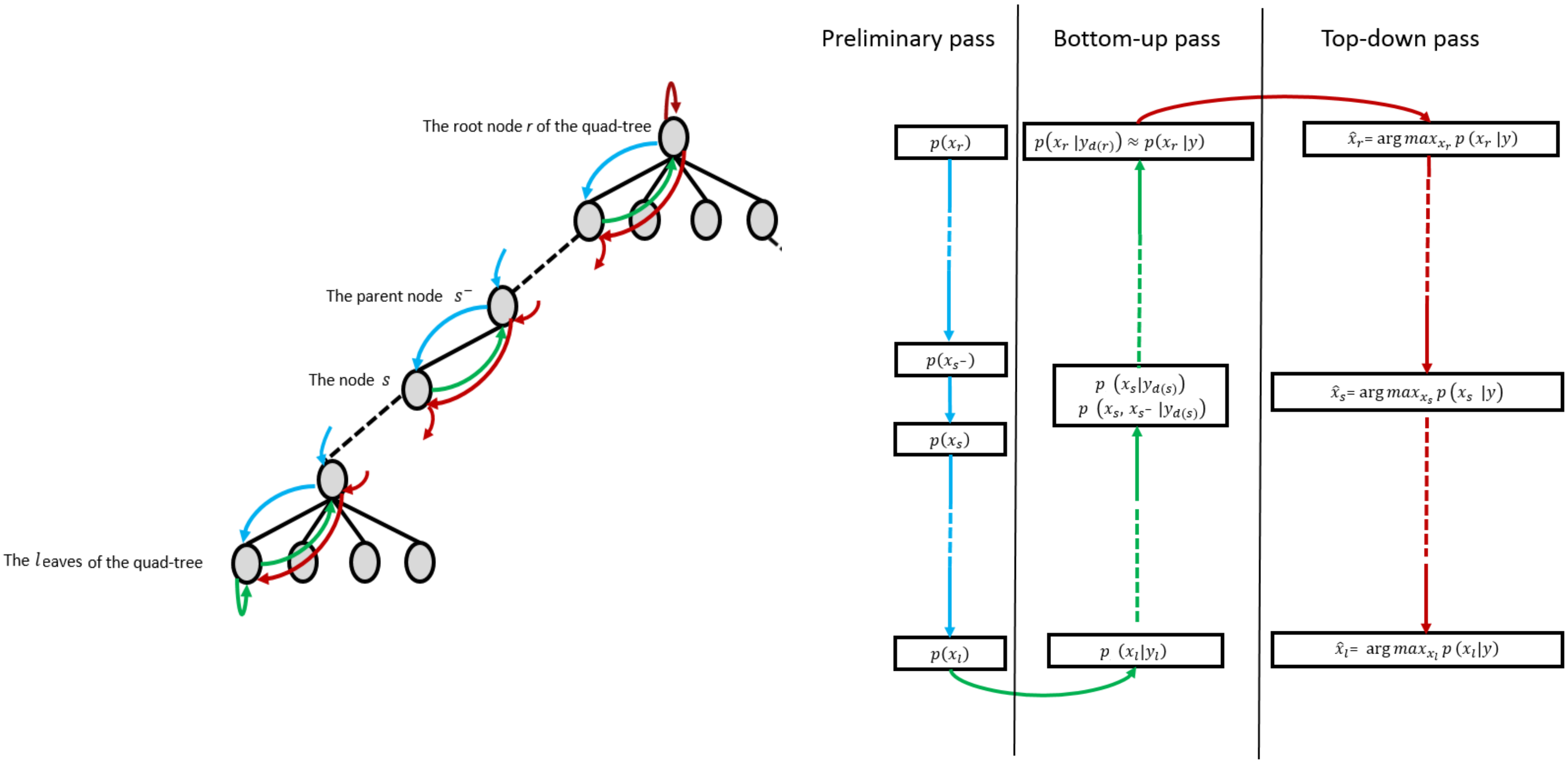

Hierarchical Markov Model on quad-trees

Blocky artifacts

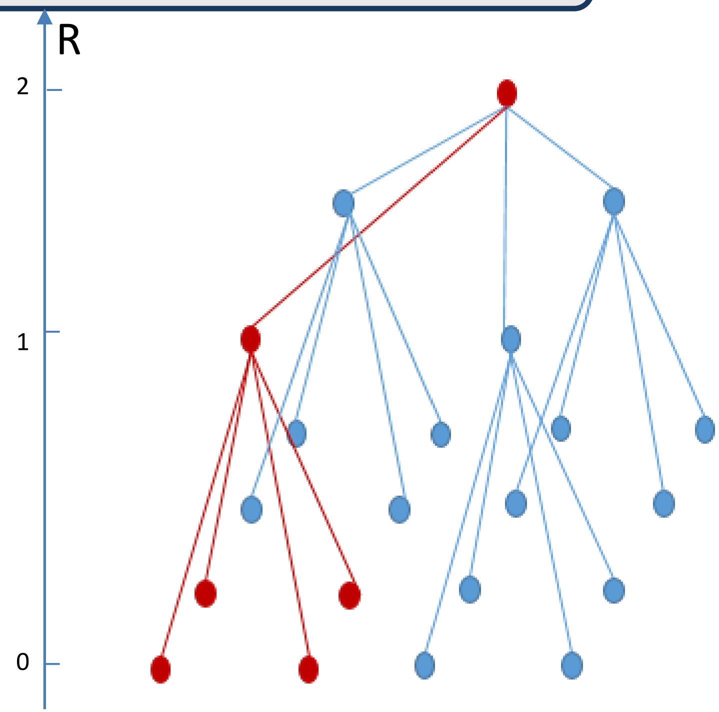

Two neighboring sites at a given scale may not have the same parent.

⇓

A **boundary** is more likely to appear than when they are linked to the same parent node.

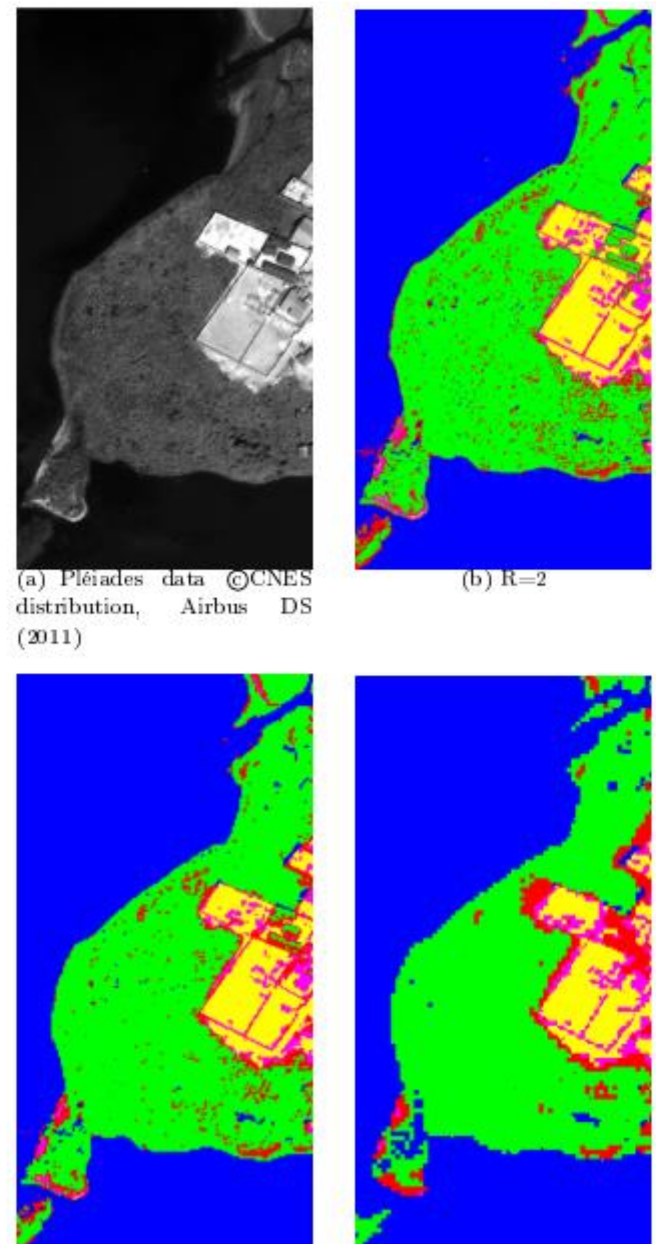

(a) Pléiades data ©CNES distribution, Airbus DS (2011)

(b) R=2

(c) R=3

(d) R=4

Contents

Multi-temporal Hierarchical Markov Model

Novel hierarchical cascade structure

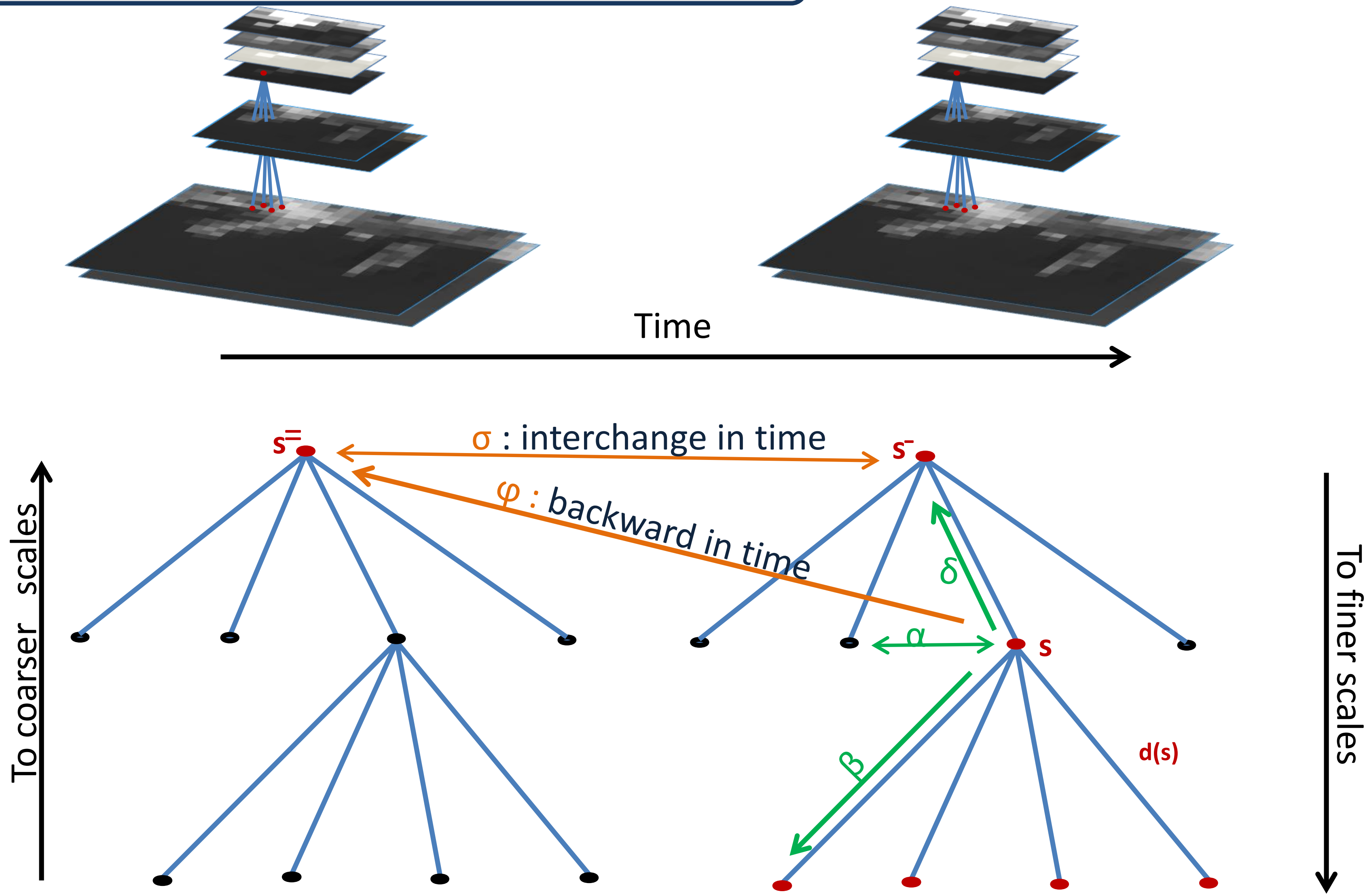

Multi-temporal Hierarchical Markov Model

MPM formulation

$$\boxed{\hat{x}_s = \arg\max_{x_s \in \omega} P(x_s \mid y)}$$

$$p(x_s \mid y) = \sum_{x_{s^-},\, x_{s^=}} \left[\frac{p\left(x_s, x_{s^-}, x_{s^=} \mid y_{d(s)}\right)}{\sum_{x_s} p\left(x_s, x_{s^-}, x_{s^=} \mid y_{d(s)}\right)} \cdot p(x_{s^-} \mid y)\, p(x_{s^=} \mid y) \right]$$

Calculate recursively the posterior marginal $p(x_s \mid y)$ while the probabilities $p\left(x_s, x_{s^-}, x_{s^=} \mid y_{d(s)}\right)$ are made available.

$$\overbrace{\underset{4}{p(x_s \mid x_{s^-}, x_{s^=})} \cdot \frac{\overset{3}{p(x_{s^-} \mid x_{s^=})} \cdot p(x_{s^=})}{p(x_s)}\,_{1} \cdot \overset{2}{p\left(x_s \mid y_{d(s)}\right)}}$$

1 Prior

2 Posterior marginal

3, 4 Transition Probabilities over scale and time

These probabilities are calculated through a MPM algorithm which runs in two passes on a quad-tree, referred to as "bottom-up" and "top-down" passes.

I. Hedhli, G. Moser, J. Zerubia, and S. B. Serpico, "A New Cascade Model for the Hierarchical Joint Classification of Multitemporal and Multiresolution Remote Sensing Data", IEEE Transactions on Geoscience and Remote Sensing (TGRS) (under revision)

Multi-temporal Hierarchical Markov Model

Time t=0: single-time MPM

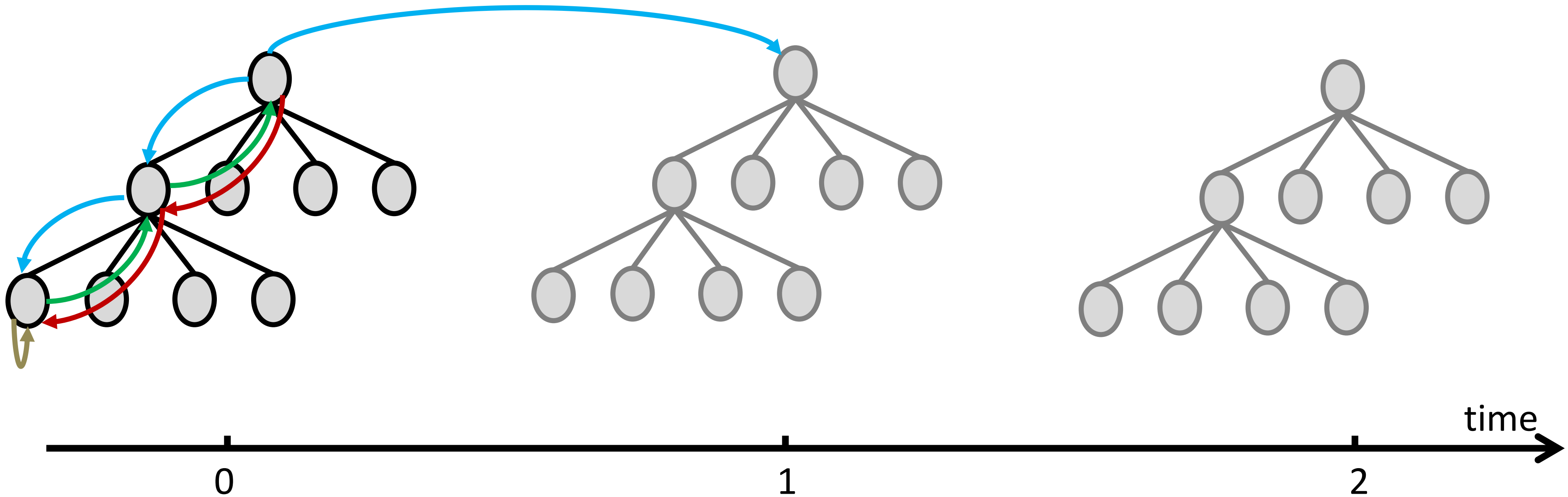

- **Classification is performed at time *t*=0 using a single-date MPM**
- **A case-specific initialization strategy is applied that makes use of a spatial MRF model**

Multi-temporal Hierarchical Markov Model

Time t=1: first top-down pass

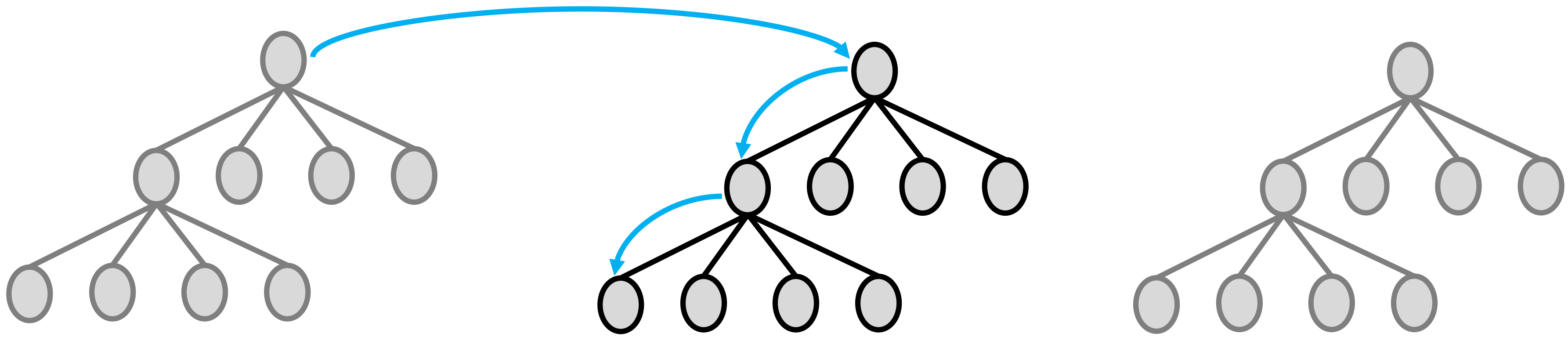

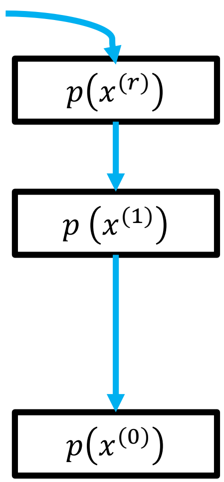

Top-down 1 Prior $p(x_s) = \sum_{x_{s^-}} \left[p(x_s \mid x_{s^-}) . \, p(x_{s^-}) \right]$

Transition Probabilities over scale*

3 $$p(x_s \mid x_{s^-}) = \begin{cases} \theta & x_s = x_{s^-} \\ \dfrac{1-\theta}{M-1} & x_s \neq x_{s^-} \end{cases}$$

Transition Probabilities over scale and time

4 $$p(x_s \mid x_{s^-}, x_{s^=}) = \begin{cases} \theta & x_s = (x_{s^-} = x_{s^=}) \\ \varphi & x_s = (x_{s^-} \neq x_{s^=}) \\ \dfrac{1-\theta}{M-1} & x_s \neq (x_{s^-} = x_{s^=}) \\ \dfrac{1-2\varphi}{M-2} & x_s \neq (x_{s^-} \neq x_{s^=}) \end{cases}$$

*C. Bouman and M. Shapiro, "A multiscale image model for Bayesian image segmentation," IEEE Trans. Image Processing, vol. 3, pp.162–177, Feb. 1994.

Multi-temporal Hierarchical Markov Model

Time t = 1: bottom-up pass

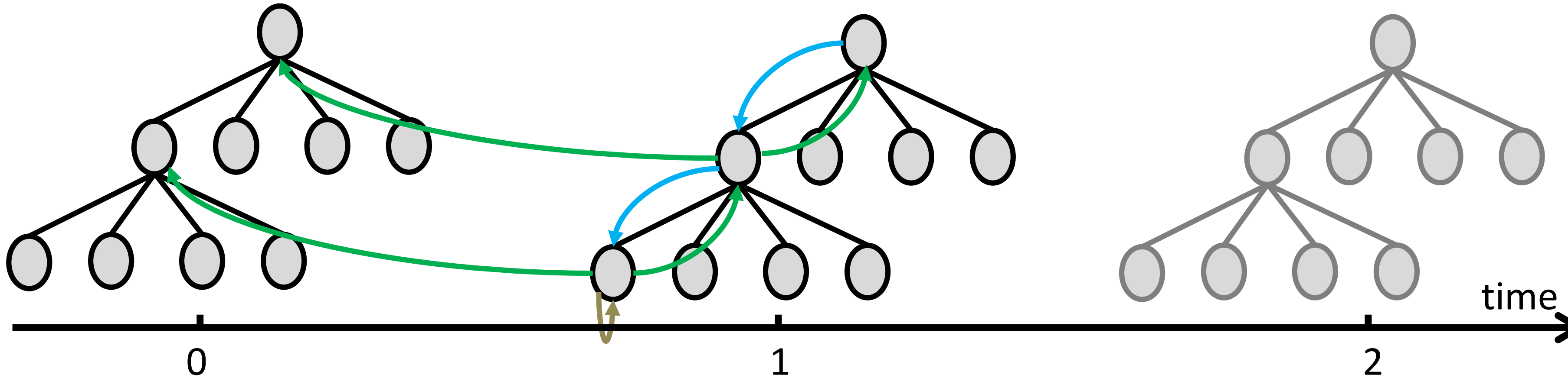

$p_2(x^{(r)})$ | $p_2(x_r \mid y_{d(s)}) = p_2(x_r \mid y\ \ )$

$p_2(x^{(1)})$ | $p_2\left(x_s^{(1)} \mid y_{d(s)}^{(1)}\right)$, $p_2\left(x_s\ \ , x_{s^-}\ x_{s^=} \mid y_s^{(1)}\right)$

$p_2(x^{(0)})$ | $p_2\left(x_s^{(0)} \mid y_s^{(0)}\right)$, $p_2\left(x_s\ \ , x_{s^-}, x_{s^=} \mid y_s^{(0)}\right)$

Bottom-up 2

Posterior marginal [4]

$$p\left(x_s \mid y_{d(s)}\right) \propto p(y_s \mid x_s).\ p(x_s).\prod_{u \in s^+} \sum_{x_u} \left[\frac{p(x_u \mid y_{d(u)})}{p(x_u)}.\ p(x_u \mid x_s)\right]$$

Likelihood term estimated using Gaussian mixture (SEM to estimate the parameters)

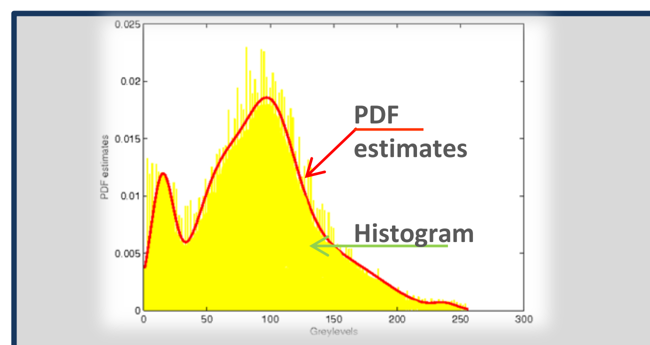

Urban area modeling

Initialisation : $p(x_s\ \ |y_s) \propto p\ (y_s|\ x_s).\ p\ (x_s\ \ )$

Multi-temporal Hierarchical Markov Model

Time t=1: second top-down pass

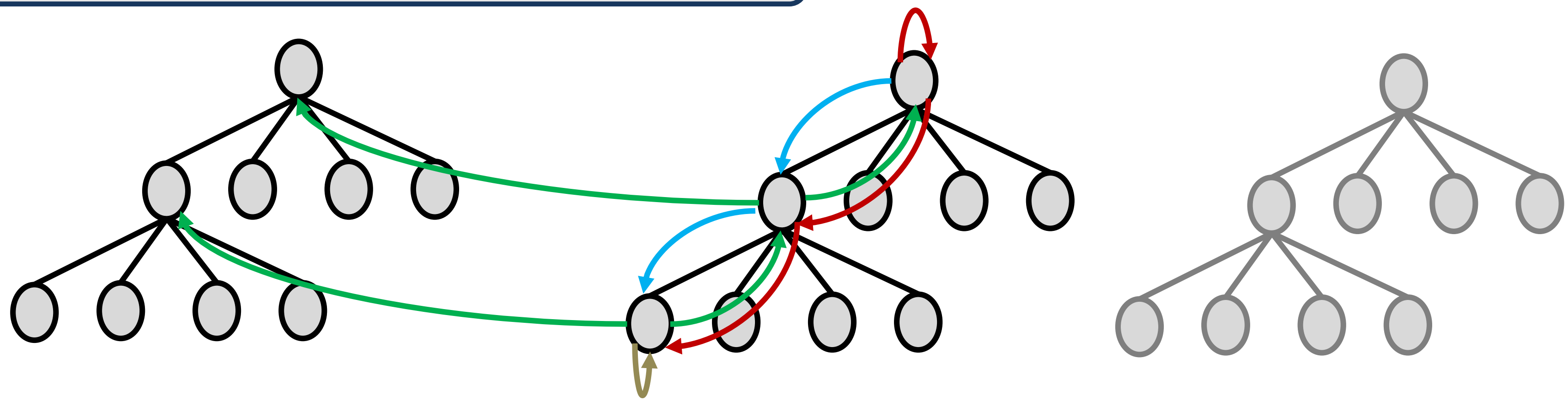

$p_2\left(x^{(r)}\right)$

$p_2\left(x^{(1)}\right)$

$p_2\left(x^{(0)}\right)$

$p_2\left(x_r \mid y_{d(s)}\right) = p_2\left(x_r \mid y \quad\right)$

$p_2\left(x_s^{(1)} \mid y_{d(s)}^{(1)}\right)$

$p_2\left(x_s \quad, x_{s^-}\ x_{s^=} \mid y_s^{(1)}\right)$

$p_2\left(x_s^{(0)} \mid y_s^{(0)}\right)$

$p_2\left(x_s \quad, x_{s^-}, x_{s^=} \mid y_s^{(0)}\right)$

$\hat{x}_r = \arg max_{x_r} \left[p\left(x_r \mid y \quad\right)\right]$

$\hat{x}_s^{(1)} = \arg max_{x_r} \left[p\left(x_s^{(1)} \mid y \quad\right)\right]$

$\hat{x}_s^{(0)} = \arg max_{x_r} \left[p\left(x_s^{(0)} \mid y \quad\right)\right]$

❖ **Need to maximize the posterior probability at each scale.**

❖ **Several techniques are used in the literature (Metropolis dynamics, ICM, Graph-cut …)**

❖ **Tool: modified Metropolis dynamics.**

Kato, Z. Zerubia, J. and Berthod, M., "Satellite image classification using a modified Metropolis dynamics," IEEE International Conference on Acoustics, Speech, and Signal Processing. ICASSP., 1992 (Volume:3) .

Experimental results

Data sets

Port au Prince
Pléiades ©CNES (2011), distribution Airbus DS

Port au Prince
Pléiades ©CNES (2012), distribution Airbus DS

Port au Prince
Pléiades ©CNES (2013), distribution Airbus DS

Port au Prince
©GeoEye (2009),

Port au Prince
©GeoEye (2010),

Experimental results


(a) Pléiades image (2013)

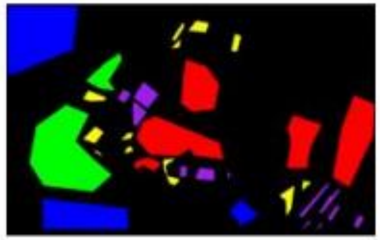
(b) Ground Truth

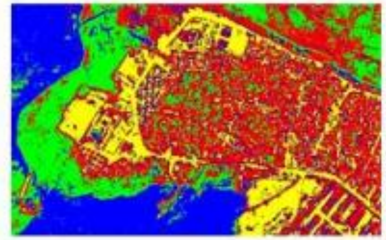
(c) Single scale method (MPM criterion)

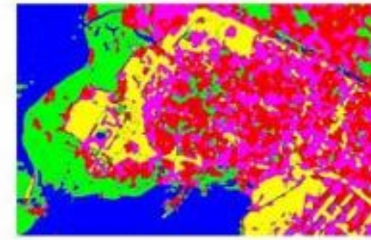
(d) Single scale method (MAP criterion)

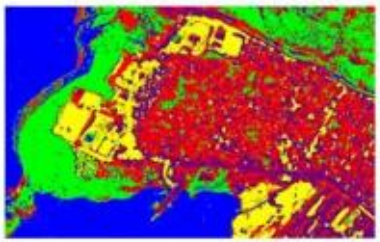
(e) Multi-temporal single scale

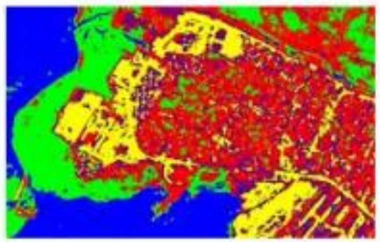
(f) The proposed method

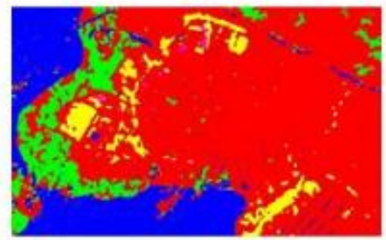
(g) KNN-MRF method

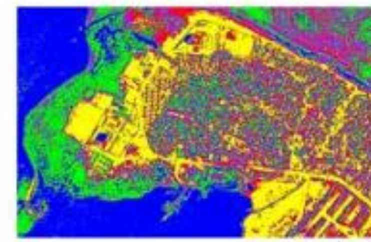
(h) Kmeans

	Port-au-Prince, Haiti						
	urban	water	vegetation	bare soil	containers	overall	computation time
Proposed method	81.62 %	100 %	90.69 %	92.82 %	62.82 %	**85,59 %**	**480 seconds**
Single scale method using MPM criterion	77.45 %	88.62 %	72.59 %	86.02 %	57.02 %	**76.34 %**	**160 seconds**
Single scale method using MAP criterion	56.14 %	100%	81,90 %	87.02%	73.21%	**79.65 %**	**220 seconds**
Multitemporal single-scale method	80.63 %	100 %	86.33 %	87.61 %	69.61 %	**84,83 %**	**≈1 hour**
K-NN + MRF	96,84%	92,42%	47.15 %	71.83 %	16.75 %	**64.99%**	**90 seconds**
K-means	12.37%	98.63%	59.18%	91.66 %	29.42 %	**58.25 %**	**20s**

Table 1. Results obtained using the Pléiades dataset: class accuracies (producer's accuracies), overall accuracy, and computation time.

Experiments were conduced using one (1600x1000) image at level 0, one (800x500) image at level 1 and four (400x250) images at level 2 on an Intel i7 quad-core (2.4 GHz) 8-GB-RAM 64-bit Linux system.

Experimental results

(a) Pléiades image (2013)

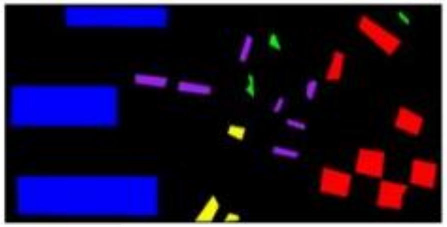

(b) Ground Truth

(c) Single scale method (MPM criterion)

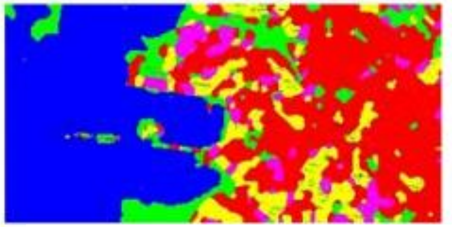

(d) Single scale method (MAP criterion)

(e) Multi-temporal single scale

(f) The proposed method

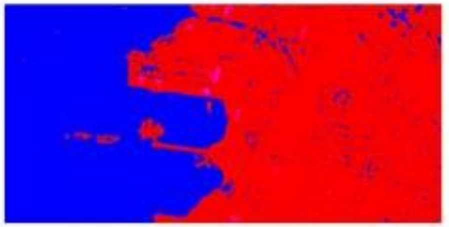

(g) KNN-MRF method

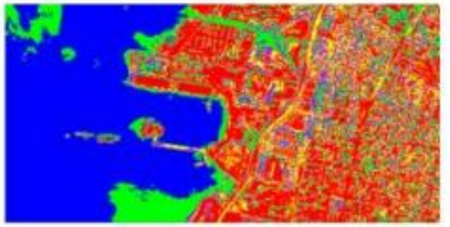

(h) Kmeans

	Port-au-Prince, Haiti						
	urban	water	vegetation	bare soil	containers	**overall**	**computation time**
Proposed method	87.59 %	100 %	98.12 %	72.82 %	82.27 %	**88,16 %**	**345 seconds**
Single scale method using MPM criterion	77.45 %	100 %	88.34 %	66.22 %	67.87 %	**79.97 %**	**90 seconds**
Single scale method using MAP criterion	64.52 %	100%	92.15 %	85.62%	49.47 %	**78.35 %**	**140 seconds**
Multitemporal single-scale method	80.63 %	100 %	89.79 %	70.54 %	74.29 %	**83,05 %**	**≈1 hour**
K-NN + MRF	100%	100%	0%	0%	12.28%	**42.45 %**	**40 seconds**
K-means	88.97%	100%	88.14%	45.6 %	36.96 %	**71.93 %**	**15 seconds**

Table 2. Results obtained using the GeoEye dataset: class accuracies (producer's accuracies), overall accuracy, and computation time.

Experiments were conduced using one (1600x800) image at level 0, one (800x400) image at level 1 and one (400x250) image at level 2 on an Intel i7 quad-core (2.4 GHz) 8-GB-RAM 64-bit Linux system.

Experimental results

✓ Blocky artifacts

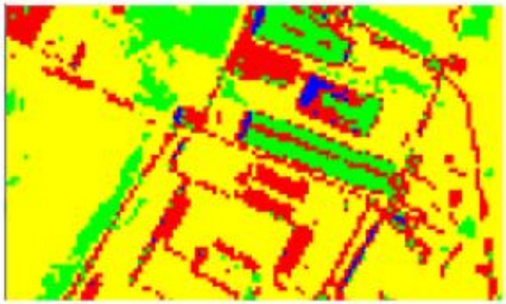

(a)

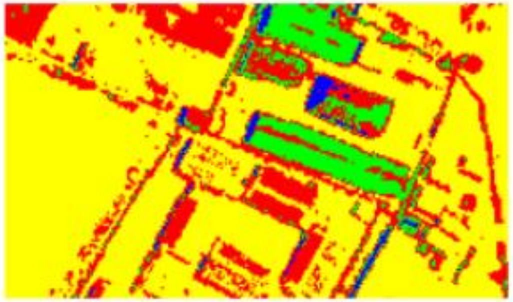

(b)

blocky artefacts using the method with a single quad-tree (MPM criterion) (a) reduction of these blocky artefacts using the proposed method (b).

✓ Computation time

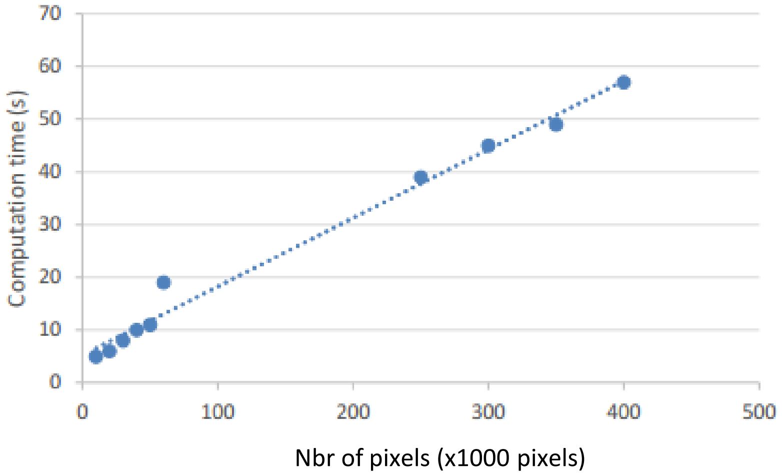

classification step

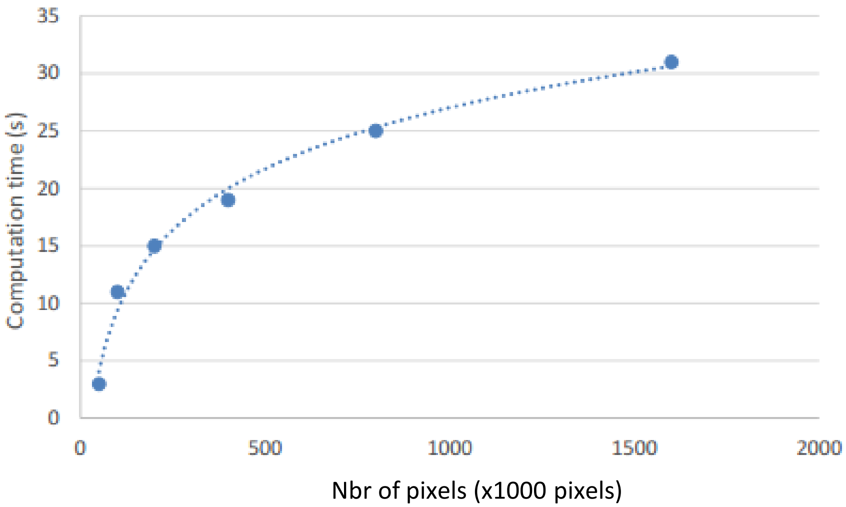

PDF estimation step

Contents

Multi-sensor Hierarchical Markov Model

The measurement in SAR and optical bands are very different from each other

How to address the problem of SAR + optical PDF modeling ?

1. First, estimate the marginal class-conditional statistics of each SAR/optical channel separately via distinct finite mixtures.
2. then, model the joint PDF through multivariate statistics.

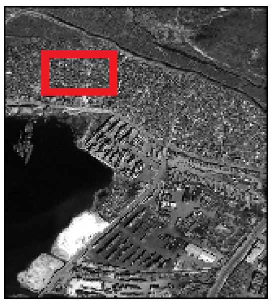

Optical data

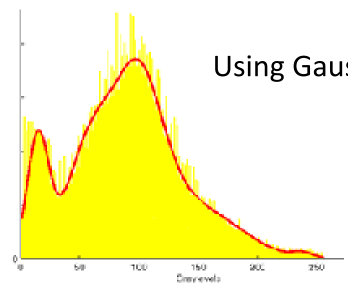

Using Gaussian mixture

multivariate statistics — Joint PDF

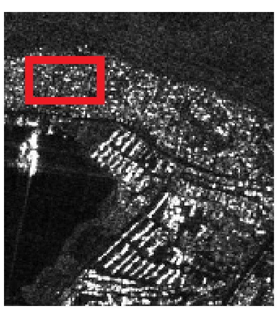

SAR data

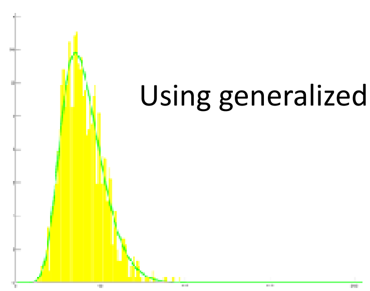

Using generalized Gamma distribution

Multi-sensor Hierarchical Markov Models

The First proposed method: highlight the synergy between two SAR sensors

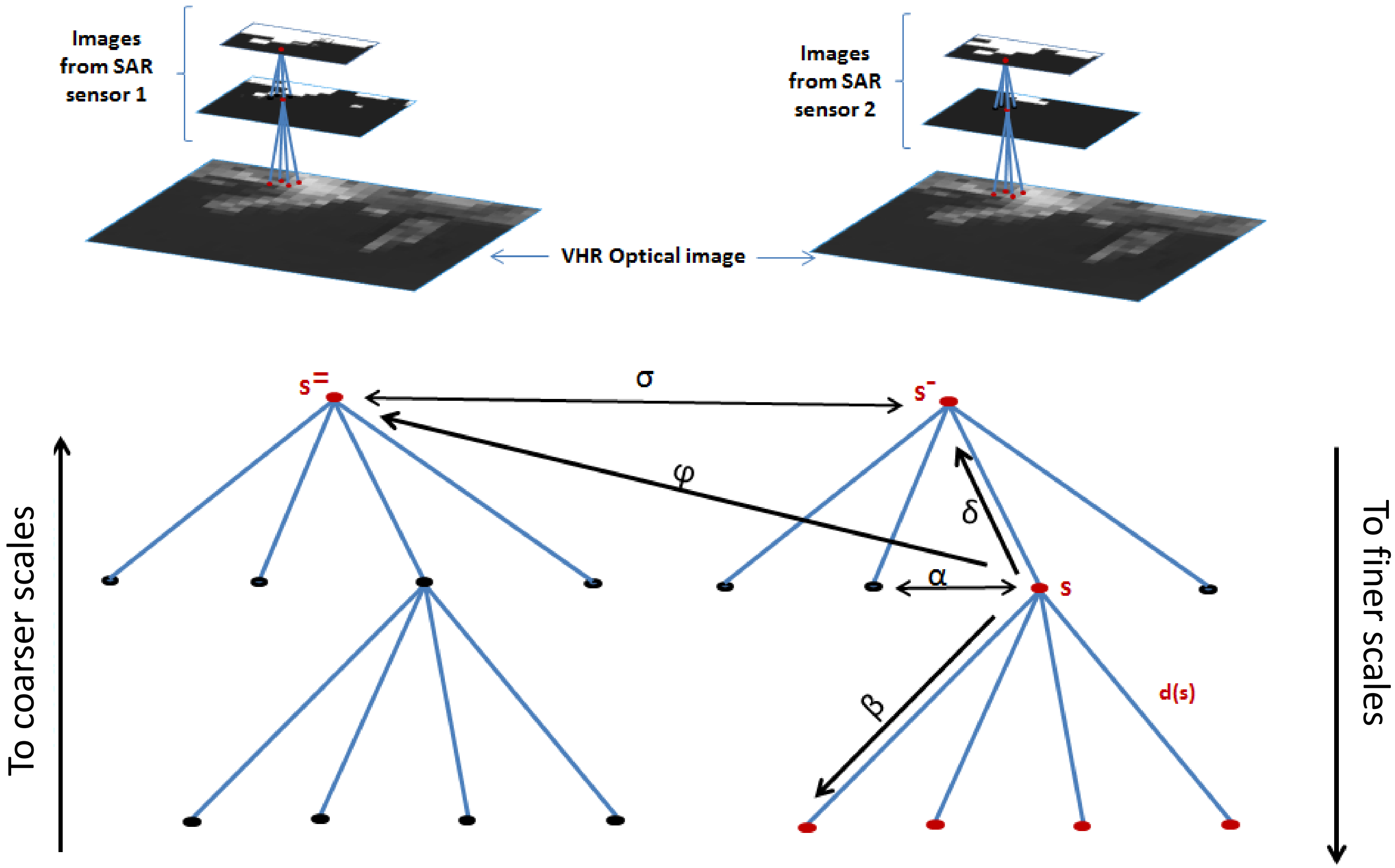

Proposed Multi-sensor Quad-tree (case 1).

Experimental results on multi-sensor data (case 1).

Figure 1

(a) (b) (c)

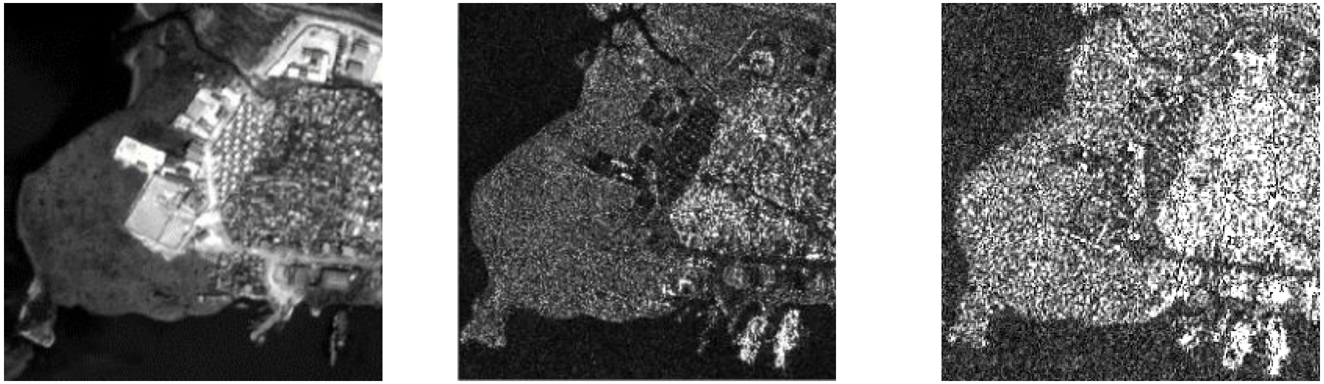

(a) Pleiades,
(b) CSK
(c) RS2

Figure 2

(a)
(b)
(c)

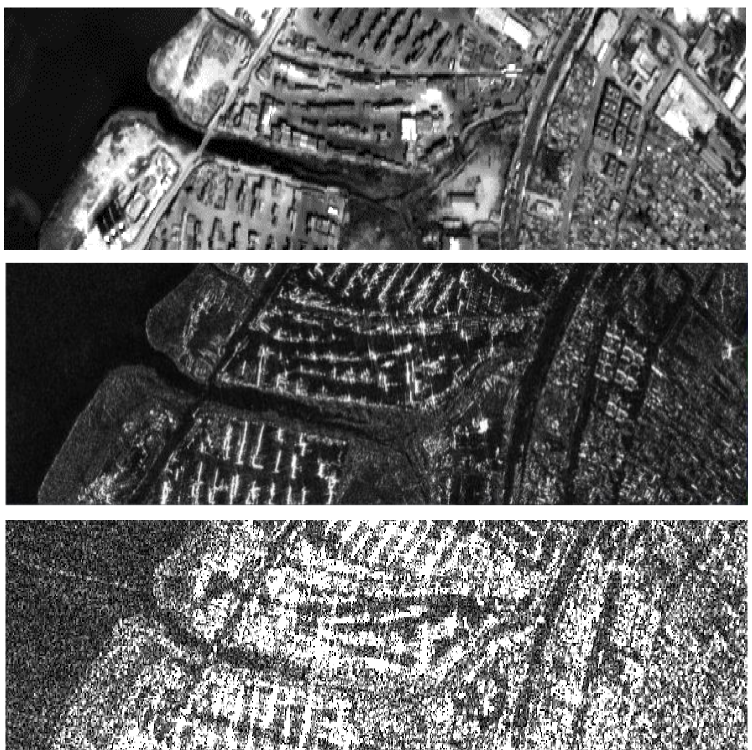

two datasets acquired over Port-au-Prince (Haiti) using:

- a panchromatic Pléiades acquisition at 0.5m resolution (Pléiades, © CNES distribution Airbus DS, 2011), shown in Figures 1(a) and 2(a).
- a CSK image (© ASI, 2011), X band, HH polarization, Spotlight mode (1m pixel spacing), geocoded, single-look, shown in Figures 1(b) and 2(b).
- a RS2 image (© CSA, 2011), C band, HH polarization, Ultra-Fine mode (1.56 m pixel spacing), geocoded, single-look, shown in Figures 1(c) and 2(c).

Experimental results on multi-sensor data (case 1).

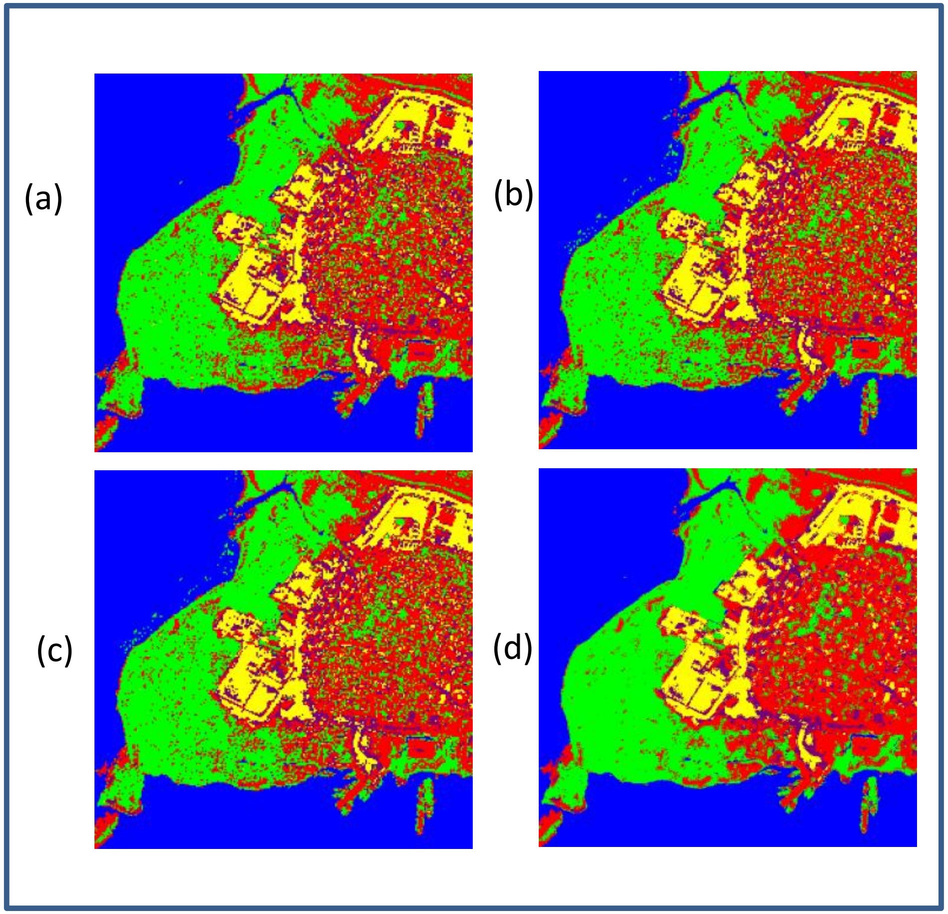

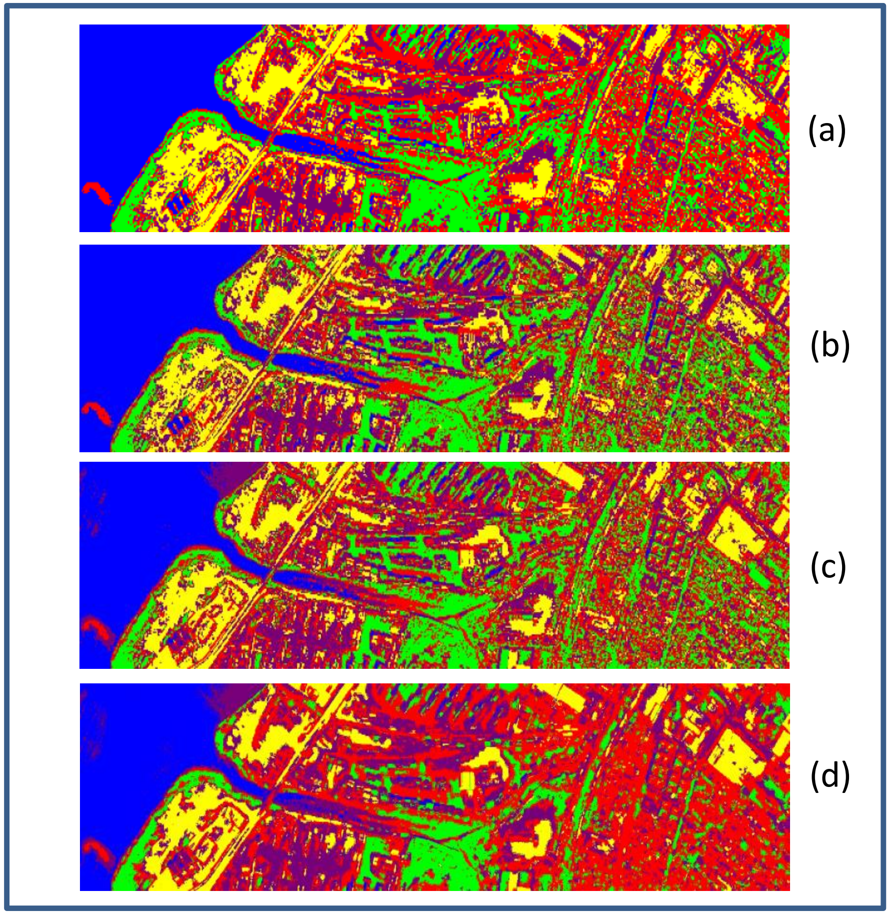

	Water	Urban	Vegetation	Bare Soil	containers	Overall accuracy
(a) Only Pléiades	100 %	61.66 %	81.69 %	82.82 %	56.72%	76.57%
(b) Pléiades + CSK	100%	44.32%	83.54%	74.75%	49.12%	70.34%
(c) Pléiades + RS2	92.56%	44.85%	79.85%	78.62%	42.15%	67.60
(d) Pléiades +CSK+RS2	90.79%	91,45 %	82,59 %	81.02 %	54.85%	80,14 %

Multi-sensor Hierarchical Markov Models

The second proposed method: SAR/optical fusion (cascade method)

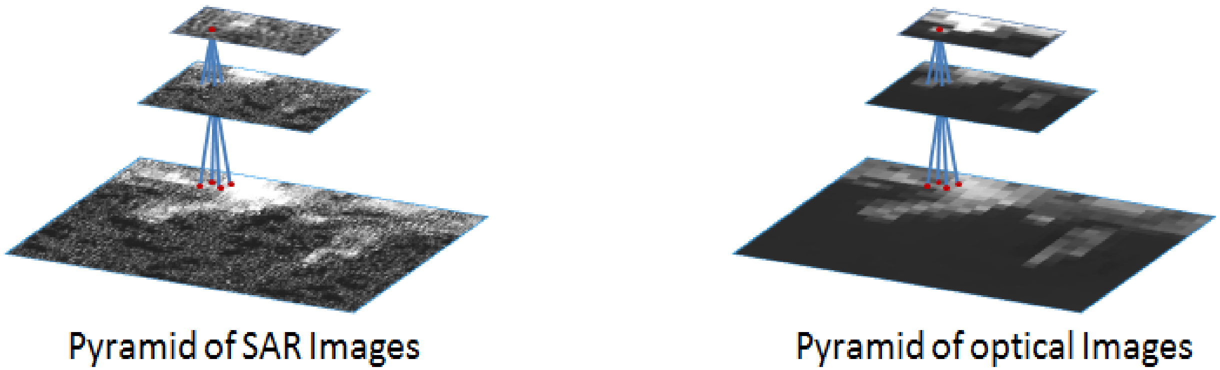

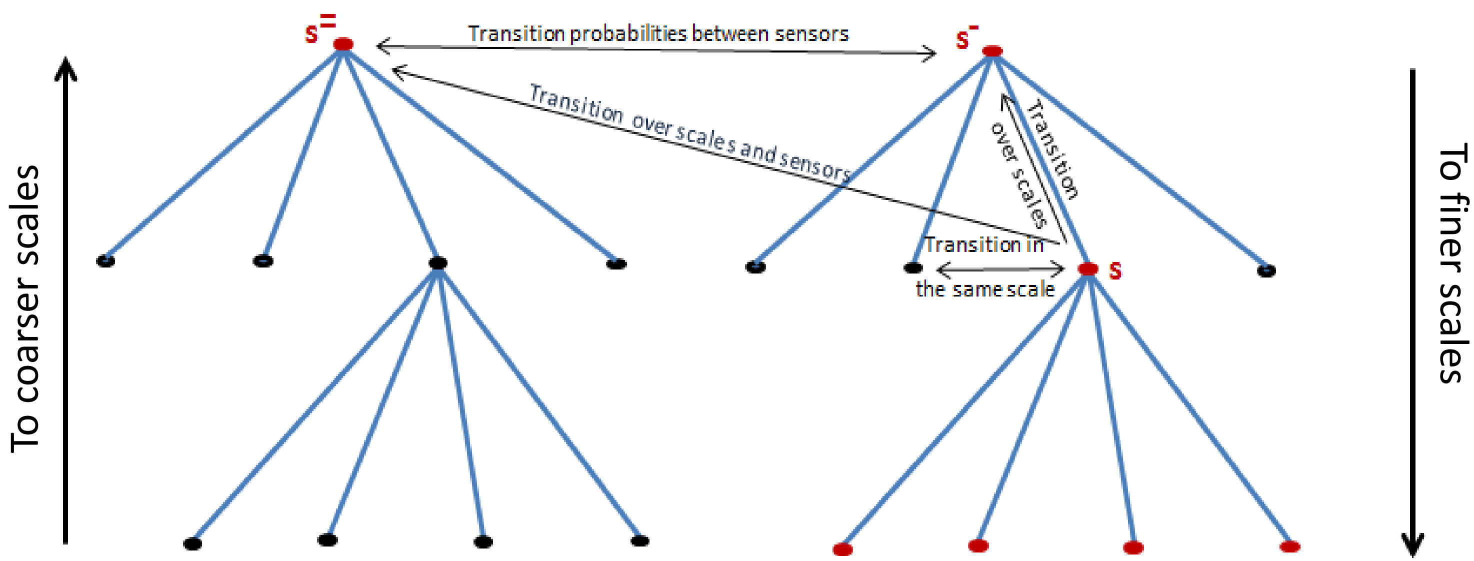

Proposed Multi-sensor Quad-tree (case 2).

Experimental results on multi-sensor data (case 2).

(a)


(b)


(c)


(d)
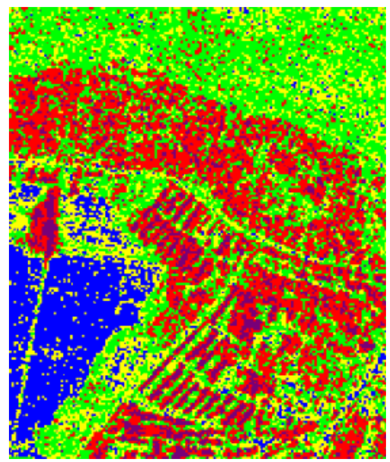

(e)
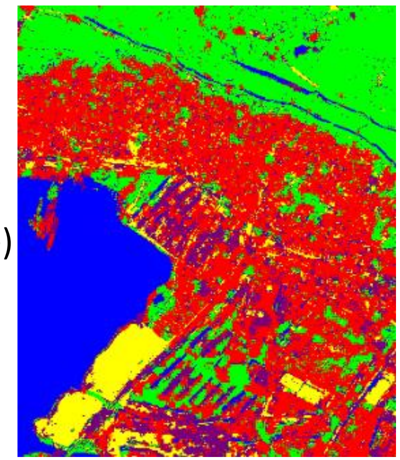

(a) One channel from the optical image (© GeoEye),
(b) SAR image (© ASI),
(c) hierarchical MRF-based classification obtained from the optical image,
(d) hierarchical MRF-based classification obtained for the SAR image,
(e) hierarchical MRF-based classification obtained by the proposed cascade method.

Contents

Contextual multi-scale classification on quad-tree

Markov Mesh Random Field (MMRF)

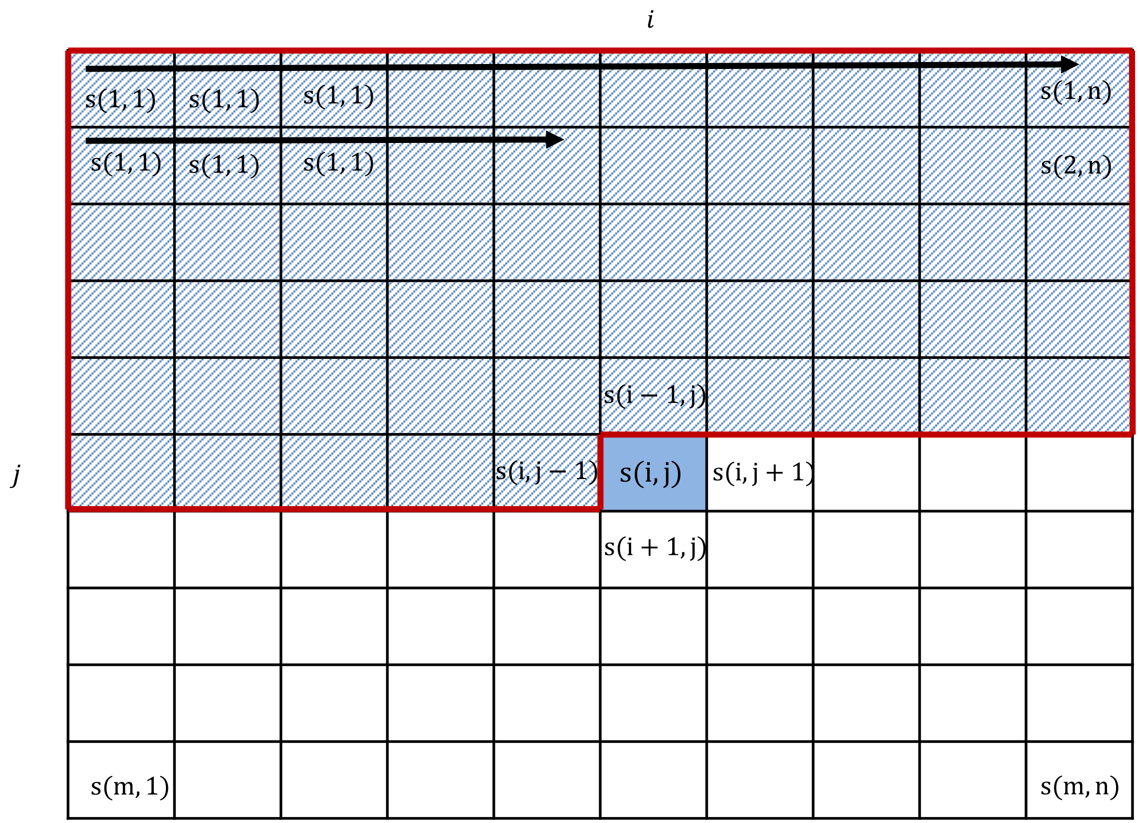

The **past** of the site $s(i, j)$ $pa(s_{i,j})$

Contextual multi-scale classification on quad-tree

Markov Mesh Random Field (MMRF)

Causal neighborhood $\partial(s_{i,j})$

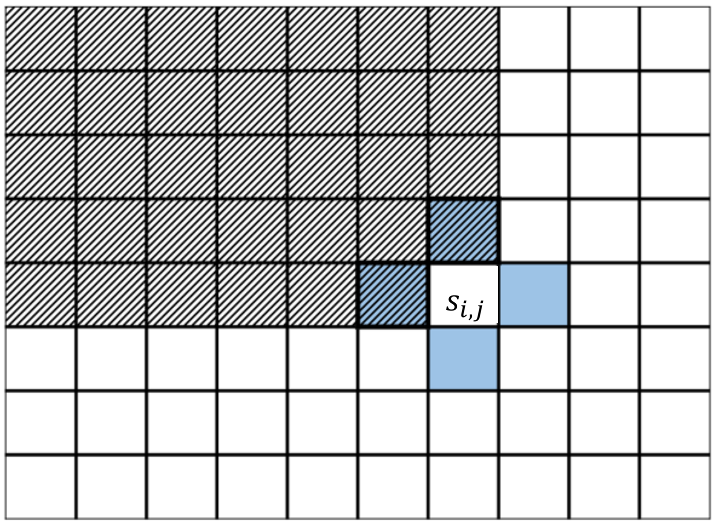

Second order MMRF

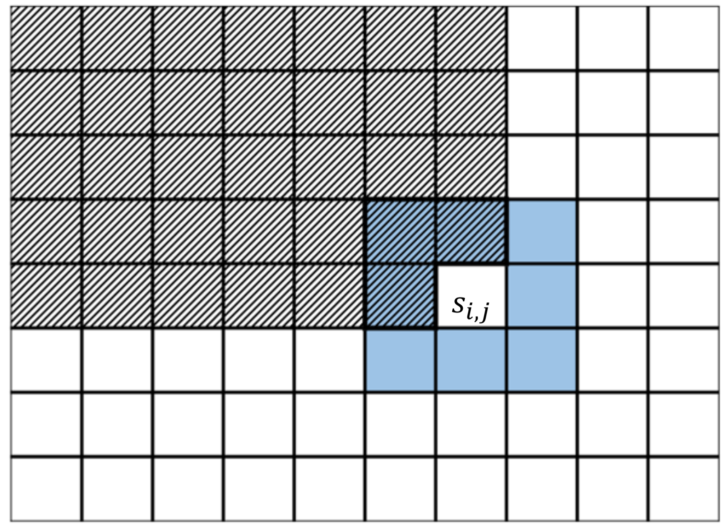

Third order MMRF

$$p\left(x_{s_{i,j}} \middle| x_{pa(s_{i,j})}\right) = p\left(x_{s_{i,j}} \middle| x_{\partial(s_{i,j})}\right) \quad (1)$$

(1) is abbreviated to: $\boxed{p(x_s|x_{pa(s)}) = p(x_s|x_{\partial(s)})}$

Hierarchical Markov Model on quad-tree

Combined Structure (MMRF and quad-tree)

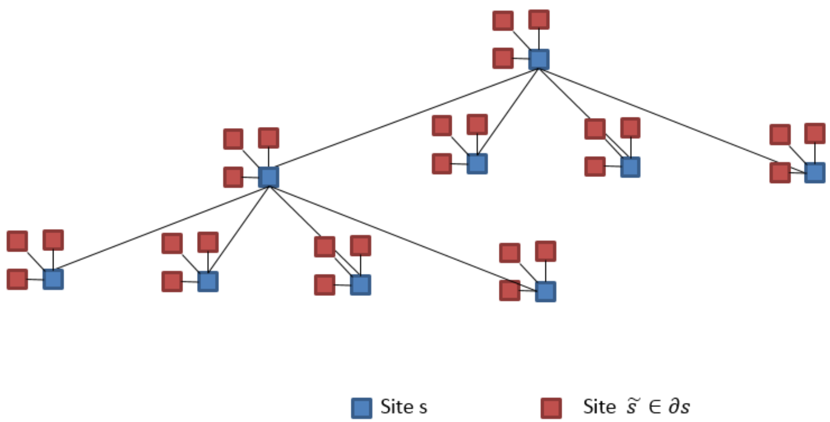

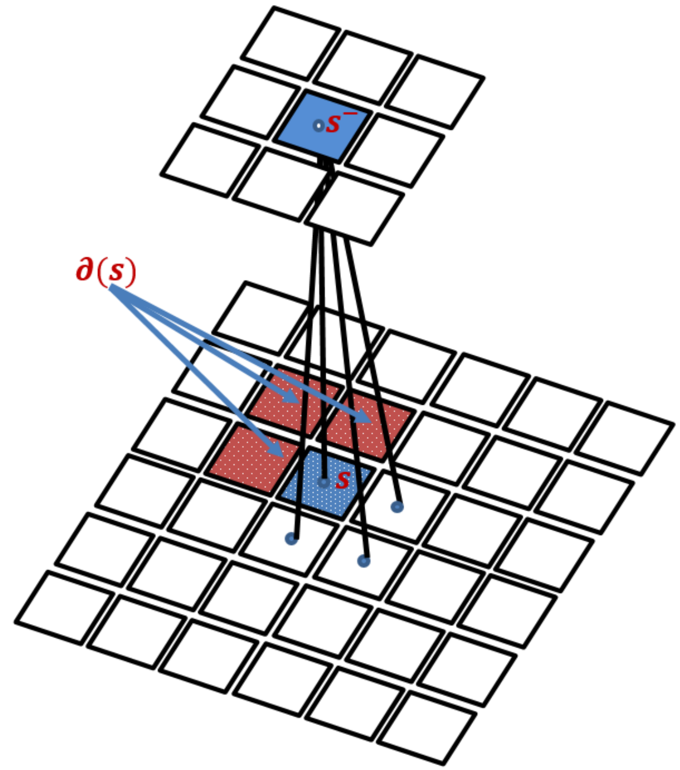

M. Basseville, A. Benveniste, K. C. Chou, S. A. Golden, R. Nikoukhah, and A. S. Willsky, “Modeling and estimation of multiresolution stochastic processes,”IEEE Trans. Inform. Theory, vol. 38, pp. 766–784, Mar. 1992.

Multi-temporal MPM inference

Again , when the **causality** property holds, **non-iterative** classification algorithms can be applied

$$\boxed{\hat{x}_s = arg \max_{x_s \in \omega} P(x_s \,|y)}$$

$$p\,(x_s\,|y\,) = \sum_{x_{s^-},\, x_{\partial(s)}} \left[\frac{p\left(x_s\,, x_{s^-}\,, x_{\partial(s)}|\, y_{d(s)}\right)}{\sum_{x_s} p\left(x_s\,, x_{s^-}\,, x_{\partial(s)}|\, y_{d(s)}\right)} \cdot p\,(x_{s^-}|y)\right] \prod_{\tilde{s}\,\in\partial(s)} p\,(x_{\tilde{s}}\,|y\,)$$

Calculate <u>recursively</u> the posterior marginal $p\,(x_s\,|y\,)$ while the probabilities $p\left(x_s\,, x_{s^-}\,, x_{\partial(s)}|\, y_{d(s)}\right)$ are made available.

$$\overbrace{\frac{\overset{3}{p\,(x_s\,|\,x_{s^-}\,)}.\, p\,(x_{s^-}\,)}{p\,(x_s\,)\ \overset{}{1}} \cdot \left[\prod_{\tilde{s}\,\in\partial(s)} \overset{4}{\frac{p\,(x_s\,|\,x_{\tilde{s}}\,).\, p\,(x_{\tilde{s}})}{p\,(x_s\,)}}\right]} \overset{2}{p\,(x_s\,|\, y_{d(s)})}$$

1 Prior

2 Posterior marginal

3 Transition Probabilities over scale

4 Contextual Probabilities

Experimental results

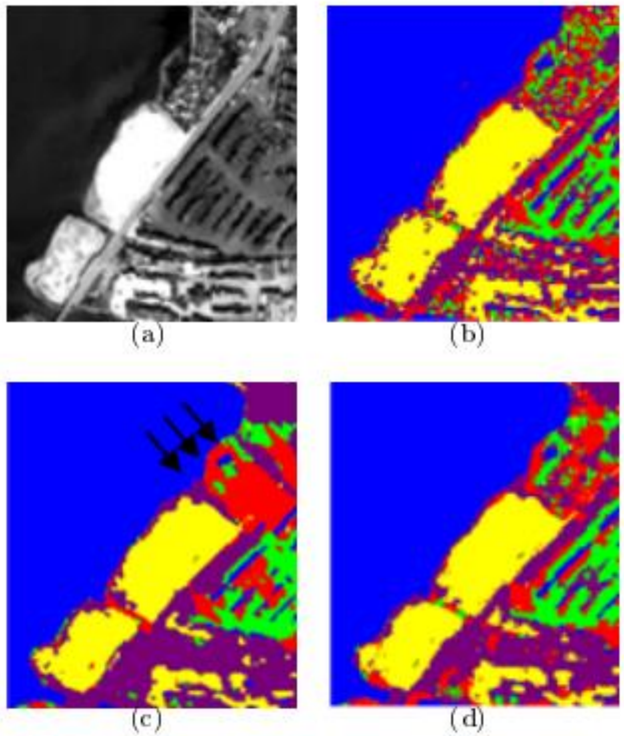

classification maps of optical(Pléiades) image (a) using the original method proposed in [Laferté et al., 2000] (b), the proposed method (c) and method in [Voisin et al., 2014] (d).

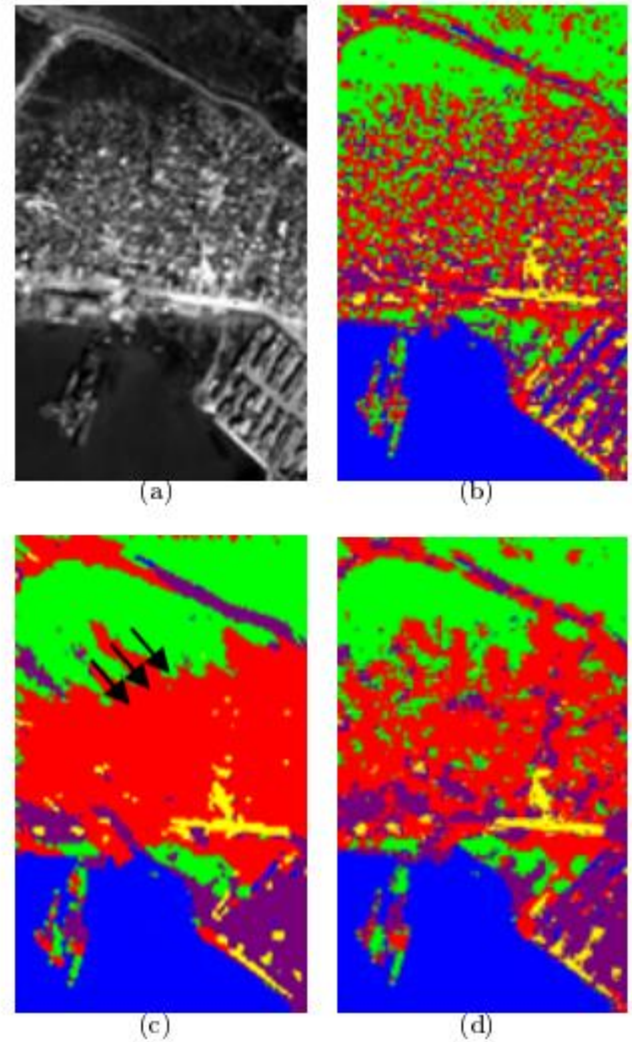

	water	urban	vegetation	containers	soil	over all	computation time
Proposed method	100	92	89	81	94	91	147 seconds
method in [Laferté et al., 2000]	100	62	76	72	91	80	120 seconds
method in [Voisin et al., 2014]	100	74	83	86	92	87	154 seconds

Contents

Conclusions

- **Methodology:**

  A family of novel techniques, framed in the methodological area of hierarchical Markov random field models, has been developed and endowed with efficient decision (MPM) and parameter estimation algorithms.

- **Application:**
  - The developed methods have been experimentally validated with complex optical multispectral, X-band SAR, and C-band SAR imagery taken from the Haiti sites.
  - The challenging problem of the classification of remote sensing images associated jointly with multiple resolutions, sensors, frequencies, and times has been addressed.

- **Results:**

  Experimental results and comparison with the state of the art suggests the effectiveness of the proposed approaches in fusing multiple information sources for classification purposes

Perspectives

- Look for an automatic selection of the **wavelet operator.**
- Propose a **new hierarchical model** in order to use a **different number of classes** at each level of the pyramid.
- Incorporate **semantic information** on class meaning at different spatial resolutions.
- Circumvent the drawback of MMRF **(corner dependency)** by using more sophisticated techniques **(QMRF, SMMRF).**
- Further optimize applicability to large data sets through **parallel processing.**

Publications

- **Peer-reviewed papers for international conferences:**

  - I. Hedhli, G. Moser, J. Zerubia and S. B. Serpico, "Contextual multi-scale image classification on quad-tree", IEEE International Conference on Image Processing (ICIP), 2016, (submitted).
  - I. Hedhli, G. Moser, J. Zerubia, and S. B. Serpico, "New hierarchical joint classification method of SAR-optical multiresolution remote sensing data", IEEE/EURASIP European Signal Processing Conference (EUSIPCO), Nice, France, Aug 2015.
  - I. Hedhli, G. Moser, J. Zerubia, and S. B. Serpico, New cascade model for hierarchical joint classification of multisensor and multiresolution remote sensing data. IEEE International Geoscience and Remote Sensing Symposium (IGARSS), Jul 2015, Milan, Italy. 2015.
  - I. Hedhli, G. Moser, J. Zerubia, and S. B. Serpico, "Fusion of multitemporal and multiresolution remote sensing data and application to natural disasters", in IEEE International Geoscience and Remote Sensing Symposium (IGARSS), Québec, Canada, July 2014.
  - I. Hedhli, G. Moser, J. Zerubia, and S. B. Serpico, "New cascade model for hierarchical joint classification of multitemporal, multiresolution and multisensor remote sensing data", in IEEE International Conference on Image Processing (ICIP), Paris, France, October 2014.

- **Peer-reviewed journals:**

  - I. Hedhli, G. Moser, J. Zerubia, and S. B. Serpico, "A New Cascade Model for the Hierarchical Joint Classification of Multitemporal and Multiresolution Remote Sensing Data", IEEE Transactions on Geoscience and Remote Sensing (TGRS) (under revision)
  - I. Hedhli, G. Moser, J. Zerubia, Nouvelle méthode en cascade pour la classification hiérarchique multi-temporelle ou multi-capteur d'image satellitaires haute résolution La Revue Française de Photogrammétrie et de Télédétection (under revision)

Acknowledgments

We would like to thank :

- ❖ The CIMA foundation (Italy) for funding the PhD scholarship.
- ❖ The French Space Agency (CNES, France) and INRIA for the financial support of travels to France and Canada.
- ❖ The French Space Agency (CNES, France) for providing the Pléiades images
- ❖ The Italian Space Agency (ASI, Italy) for providing the COSMO-SkyMed images
- ❖ The Canadian Space Agency (CSA, Canada) for providing the RADARSAT-2 images
- ❖ GeoEye Inc. and Google crisis response for providing the GeoEye images.